

## Structure of $^{22}\text{N}$ and the $N = 14$ subshell

C. Rodríguez-Tajes,<sup>1,\*</sup> D. Cortina-Gil,<sup>1</sup> H. Álvarez-Pol,<sup>1</sup> T. Aumann,<sup>2</sup> E. Benjamim,<sup>1</sup> J. Benlliure,<sup>1</sup> M. J. G. Borge,<sup>3</sup> M. Caamaño,<sup>1</sup> E. Casarejos,<sup>1,†</sup> A. Chatillon,<sup>2,‡</sup> L. V. Chulkov,<sup>2,4</sup> K. Eppinger,<sup>5</sup> T. Faestermann,<sup>5</sup> M. Gascón,<sup>1</sup> H. Geissel,<sup>2</sup> R. Gerhåuser,<sup>5</sup> B. Jonson,<sup>6,7</sup> R. Kanungo,<sup>8</sup> R. Krücken,<sup>5</sup> T. Kurtukian,<sup>1,§</sup> K. Larsson,<sup>6</sup> P. Maierbeck,<sup>5</sup> T. Nilsson,<sup>6</sup> C. Nociforo,<sup>2</sup> Yu. Parfenova,<sup>9</sup> C. Pascual-Izarra,<sup>3</sup> A. Perea,<sup>3</sup> D. Pérez-Loureiro,<sup>1</sup> A. Prochazka,<sup>2</sup> S. Schwertel,<sup>5</sup> H. Simon,<sup>2</sup> K. Sümmerner,<sup>2</sup> O. Tengblad,<sup>3</sup> H. Weick,<sup>2</sup> M. Winkler,<sup>2</sup> and M. V. Zhukov<sup>6</sup>

<sup>1</sup>Universidad de Santiago de Compostela, E-15782 Santiago de Compostela, Spain

<sup>2</sup>GSI Helmholtzzentrum für Schwerionenforschung, D-64291 Darmstadt, Germany

<sup>3</sup>Instituto de Estructura de la Materia, CSIC, E-28006 Madrid, Spain

<sup>4</sup>Kurchatov Institute, Ru-123182 Moscow, Russia

<sup>5</sup>Physik Department E12, Technische Universität München, D-85748 Garching, Germany

<sup>6</sup>Fundamental Fysik, Chalmers Tekniska Högskola, S-41296 Göteborg, Sweden

<sup>7</sup>PH Department, CERN, CH-1211 Geneva 23, Switzerland

<sup>8</sup>Astronomy and Physics Department, Saint Mary's University, Halifax, NS B3H 3C3, Canada

<sup>9</sup>Flerov Laboratory of Nuclear Reactions, JINR, 141980 Dubna, Russia

(Received 8 February 2011; revised manuscript received 11 May 2011; published 13 June 2011)

One-neutron knockout data for  $^{18-22}\text{N}$  are analyzed in the eikonal approximation of the Glauber model. The role of the  $s$ - $d$  shell and the crossing of the  $N = 14$  neutron subshell are discussed. Of particular interest is the nucleus  $^{22}\text{N}$ , where the knockout data provide a sensitive experimental test for a possible halo structure of its ground state. The observation of a narrow momentum distribution of the  $^{21}\text{N}$  fragments, together with an essential  $1s_{1/2}$  contribution needed to describe the observed longitudinal-momentum distribution, allow the firm conclusion that the ground state of  $^{22}\text{N}$  is a well-developed nuclear halo. The results also show that the  $N = 14$  subshell in  $^{22}\text{N}$  is somewhat reduced as compared to that of  $^{23}\text{O}$ .

DOI: [10.1103/PhysRevC.83.064313](https://doi.org/10.1103/PhysRevC.83.064313)

PACS number(s): 21.10.Gv, 21.10.Pc, 21.60.Cs, 27.20.+n

### I. INTRODUCTION

There has recently been a renewed interest in the structure of the most neutron-rich oxygen isotopes, both experimentally and theoretically. The absence of bound oxygen isotopes beyond  $N = 16$  is well known, but the question of whether there is a shell closure at this neutron number has only lately been established. Neutron-knockout reactions showed early on [1] that the valence neutron in  $^{23}\text{O}$  mainly occupied the  $1s_{1/2}$  orbit, and results from a recent similar experiment for  $^{24}\text{O}$  [2] showed that the last two neutrons are in an almost pure  $(1s_{1/2})^2$  configuration. This fact, together with the observation of the first excited  $2^+$  state in  $^{24}\text{O}$  [3] at 4.7 MeV, gives firm proof of an unconventional shell closure at  $N = 16$ . In this work, a related problem is addressed, namely, the role of the  $1s_{1/2}$  orbit for the structure of  $^{22}\text{N}$ , which is the isotone of  $^{23}\text{O}$ . This is done in a theoretical analysis of the experimental momentum distributions of fragments after one-neutron knockout reactions from a chain of nitrogen isotopes measured at GSI [4,5], ranging from  $A = 18$  to 22. The role of the  $s$ - $d$  shell and the crossing of the  $N = 14$  neutron number are discussed with special emphasis on the possible halo structure of  $^{22}\text{N}$ .

The first observation of  $^{22}\text{N}$ , with isospin projection of 4, was done by Westfall *et al.* [6] in the pioneering nuclear fragmentation experiments with a 212 MeV/nucleon  $^{48}\text{Ca}$  beam. Its half life, the beta-delayed neutron-emission probabilities  $P_n$  [7], and its mass [8] were measured at the Grand Accélérateur National d'Ions Lourds (GANIL). The production cross section for  $^{22}\text{N}$ , using a relativistic  $^{40}\text{Ar}$  primary beam, was measured at GSI as 23.9(7.3) nb [9]. The interaction cross section of  $^{22}\text{N}$  was determined to be 1245(49) mb [10], which was interpreted as an extended matter distribution in the  $^{22}\text{N}$  ground state [11]. The reaction cross section and strong absorption radius were explored for neutron-rich light nuclei, including  $^{22}\text{N}$ , by Khouaja *et al.* [12]. Detailed in-beam gamma spectroscopy, based on the use of two-step reactions, was performed by Sohler *et al.* [13] and provided decay schemes for the neutron-rich nitrogen isotopes, including the case of  $^{22}\text{N}$ . Strongman *et al.* [14] studied neutron-unbound states in  $^{22}\text{N}$ , and drew some conclusions about a possible reduction of the  $N = 14$  shell gap for the nitrogen chain. Finally, a recent experiment at the National Superconducting Cyclotron Laboratory (NSCL) [15] measured the  $\beta$  decay of  $^{22}\text{N}$ , determining the complex level scheme of its daughter,  $^{22}\text{O}$ . These data also showed a large Gamow-Teller strength to a highly excited state in  $^{22}\text{O}$ , in analogy with the  $\beta$  decay of the two-neutron halo nucleus  $^{11}\text{Li}$  to an excited state in  $^{11}\text{Be}$  at 18.5 MeV [16].

### II. EXPERIMENT

The experimental data for  $^{18-22}\text{N}$  analyzed in this work were obtained in the experiment performed with the fragment

\*Present address: Centro de Láseres Pulsados Ultracortos Ultraintensos, E-37008 Salamanca, Spain; carme.rodriguez@usal.es.

†Present address: Universidade de Vigo, E-36310 Vigo, Spain

‡Present address: CEA/DAM, Bruyères-le-Châtel, F-91290 Aapajon Cedex, France.

§Present address: Centre d'Études Nucléaires de Bordeaux Gradignan, F-33175 Gradignan, France.

separator (FRS) spectrometer [17] at GSI. The nitrogen isotopes were produced in projectile fragmentation of a fully ionized  $^{40}\text{Ar}$  primary beam, accelerated in the heavy-ion synchrotron (SIS) to 700 MeV/nucleon and then impinging on a  $4\text{ g/cm}^2$  Be target placed at the entrance of the FRS. The nitrogen isotopes were separated in the first half of the FRS. A reaction target of  $1720\text{ mg/cm}^2$   $^9\text{Be}$  was placed at the intermediate focal plane and the analysis of the one-neutron knockout fragments was performed in the second half of the FRS. Details of the experimental setup and the analysis procedure can be found in [4,5].

### III. RESULTS

The results obtained for the one-neutron removal cross sections and longitudinal-momentum distributions of the  $A-1$  fragments are summarized in Table I. A special comment is needed to understand how the cross sections were obtained. They were directly calculated from the ratio between the number of incident projectiles and the fragments passing through the FRS. This ratio was corrected for the limited transmission, the detection efficiency, and the contributions from secondary reactions in the material surrounding the reaction target. The experimental values for the latter contribution were measured in the cases  $^{18-20}\text{N}$  by running the experiment without target, and are taken into account in the third column of Table I. The corrections for the heavier nitrogen isotopes,  $^{21,22}\text{N}$ , were then extrapolated and were taken as a 30% reduction. The widths deduced from the measured longitudinal-momentum distributions are given in the fourth column of Table I. Note that there are changes in the numerical values with respect to Ref. [5], since a more realistic Glauber-type model was adopted in this work.

The theoretical interpretation of the results presented above is done using calculations performed in the eikonal approximation of the Glauber model. Such an approach is justified since the data discussed here were obtained at high energy, where the eikonal approximation [18] is the proper theoretical tool. This is thus a convenient approach for the description of the momentum distributions of the core

TABLE I. Experimental values of the inclusive one-neutron knockout cross sections and widths of the fragment longitudinal-momentum distributions. For those entries labeled as \* in the third column, no empty-target measurements were available and the corrections of the cross sections were extrapolated. The full width at half maximum (FWHM) values given in the fourth column differ slightly from the ones published in Ref. [5] because more accurate descriptions of the longitudinal-momentum distributions were used in this work.

Isotope	$\sigma_{-1n}$ (mb)	$\sigma_{-1n}^{\text{corrected}}$ (mb)	FWHM (MeV/c)
$^{18}\text{N}$	$89 \pm 9$	$64 \pm 9$	$128 \pm 8$
$^{19}\text{N}$	$90 \pm 10$	$65 \pm 10$	$160 \pm 4$
$^{20}\text{N}$	$105 \pm 13$	$71 \pm 13$	$175 \pm 16$
$^{21}\text{N}$	$112 \pm 16$	$79 \pm 16^*$	$160 \pm 32$
$^{22}\text{N}$	$137 \pm 34$	$97 \pm 34^*$	$77 \pm 32$

fragments and the corresponding cross sections in one-nucleon stripping. The method has been discussed earlier [18] and has been used successfully in calculations of, for example, the  $^9\text{Be}$  ( $^{11}\text{Be}$ ,  $^{10}\text{Be}$ ) reaction [19,20]. In this model, the determination of realistic profile functions  $S_i$  ( $i = \text{core}, n$ ), and the core-nucleon wave functions are the major points for the calculations. In the present analysis, the wave functions were obtained as solutions of the Schrödinger equation with a Woods-Saxon potential, which is well suited for one-neutron halo systems. The width of the potential was chosen equal to the rms radius of the nucleus, given in Ref. [10]. The depth of the potential was fitted to the valence-neutron separation energy. The profile function was calculated using  $NN$  cross sections, as in Ref. [21]. The Be target-density distribution was approximated within the harmonic oscillator model (see Ref. [22]) with the parameters  $a = 1.694\text{ fm}$  and  $\alpha = 0.549$ . The core-density distribution was approximated by a two-parameter Fermi model [22], fitted to reproduce the core-target interaction cross section, given in [10]. The interaction cross section of the excited core was calculated as the cross section of the system with mass  $(A-2)$  plus one neutron.

Generally, the structure of nitrogen isotopes, with an odd number of protons, is substantially more complicated than the case of even-proton-number isotopes (i.e., oxygen). For the heavy nitrogen isotopes, the seventh proton occupies the  $0p_{1/2}$  orbit, while the neutrons in all cases belong to the  $s$ - $d$  shell, which results in negative parity states for all of the explored configurations.

A summary of the theoretical fits to the data is presented in Table II for  $^{18-22}\text{N}$ . The spin and parity of the analyzed nuclei are included in the first column. The second and third columns give the energy and spin parity of the core states included in the fit. The fifth column gives the orbital angular momentum of the neutron that is assumed to be coupled to the different core configurations. The last column gives the relative weights of the contributions from the ground state and the first excited state of the core obtained from the fits

TABLE II. Calculated contributions of core ( $E_{\text{core}}, I_{\text{core}}^\pi$ )  $\otimes n(l)$  configurations in the structure of  $^{18-22}\text{N}$  isotopes. The fourth column gives references to the level schemes of the core nuclei used in the calculations. The errors given in the sixth column were directly obtained from the fit of the experimental data to the theoretical distributions and do not include model dependences.

Isotope ( $I^\pi$ )	$E_{\text{core}}$ (MeV)	$I_{\text{core}}^\pi$	Ref.	l	Weight
$^{18}\text{N}$ ( $1^-$ )	0.0	$1/2^-$	[23]	0	$0.31 \pm 0.01$
	1.37	$3/2^-$		2	$0.69 \pm 0.01$
$^{19}\text{N}$ ( $1/2^-$ )	0.0	$1^-$	[24]	0	$0.31 \pm 0.01$
	0.115	$2^-$		2	$0.69 \pm 0.01$
$^{20}\text{N}$ ( $2^-$ )	0.0	$1/2^-$	[13]	2	$0.83 \pm 0.03$
	1.143	$3/2^-$		0	$0.17 \pm 0.03$
$^{21}\text{N}$ ( $1/2^-$ )	0.0	$2^-$	[13]	2	$0.68 \pm 0.03$
	1.336	$1^-$		0	$0.32 \pm 0.03$
$^{22}\text{N}$ ( $0^-$ ) <sup>a</sup>	0.0	$1/2^-$	[13]	0	$0.45 \pm 0.10$
	1.177	$3/2^-$		2	$0.55 \pm 0.10$
$^{22}\text{N}$ ( $0^-$ ) <sup>b</sup>	0.0	$1/2^-$	[13]	0	$0.48 \pm 0.10$
	2.405	$5/2^-$		2	$0.52 \pm 0.10$

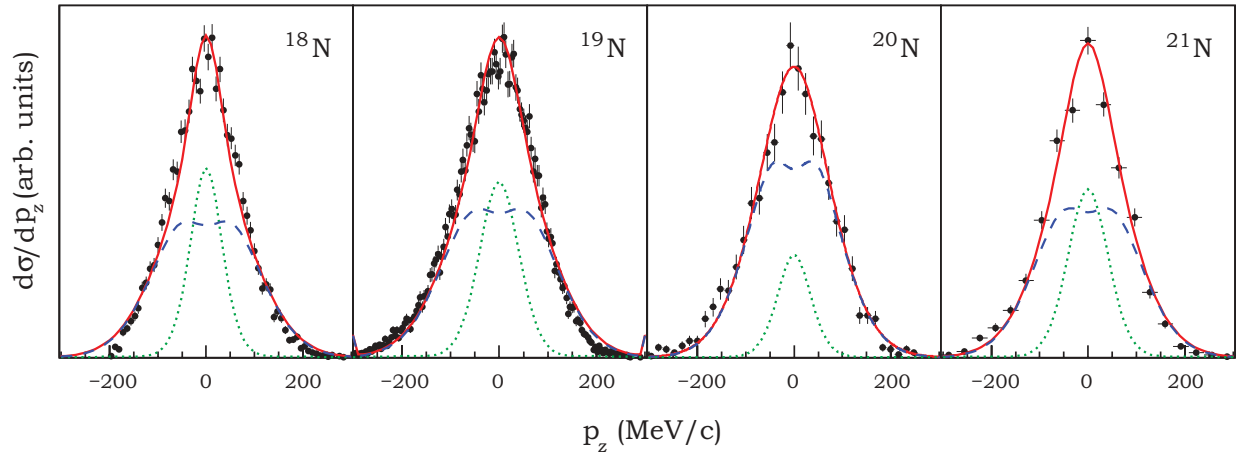


FIG. 1. (Color online) Longitudinal-momentum distributions of fragments after neutron-knockout of  $^{18-21}\text{N}$ . The curves correspond to theoretical calculations in an eikonal Glauber model folded with the experimental resolution. The dotted and dashed lines correspond to the coupling of the core to an  $s_{1/2}$  and a  $d_{5/2}$  neutron, respectively, and the solid curve to their sum.

to the data. These weights give part of the total one-neutron removal cross section (in Table I) connected to the ground-state or excited-state coupling. In the case of  $^{22}\text{N}$ , two cases were considered: first, the coupling to the first excited state of  $^{21}\text{N}$ , with  $I^\pi = 3/2^-$ , referred to as case (a), and second, the coupling to the second excited state in  $^{21}\text{N}$ , with  $I^\pi = 5/2^-$ , referred to as case (b). Figure 1 shows the results of the fits for  $^{18-21}\text{N}$ . For  $^{18,19}\text{N}$ , the main contribution comes from a  $d_{5/2}$  neutron coupled to an excited state of the core. For the cases  $^{20,21}\text{N}$ , with one and two additional neutrons, this trend

is broken so that the strongest component of the wave function instead comes from a  $d_{5/2}$  neutron coupled to the ground state of the corresponding core.

Figure 2 shows the result of the fit to the  $^{22}\text{N}$  data for the case (a) in Table II, where a  $s_{1/2}$  neutron is coupled to the ground state of the  $^{21}\text{N}$  core and a  $d_{3/2}$  neutron is coupled to the first excited state, at 1.177 MeV. A separate figure is not included for the case (b), where the coupling of a  $d_{5/2}$  neutron to the second excited state of  $^{21}\text{N}$  was considered, since there is no observable difference. The contributions from the coupling to the ground state and the first (second) excited state of the core have roughly equal probabilities. It should be pointed out here that without the measurement of gamma-ray coincidences, it is not possible to distinguish between the cases (a) and (b).

#### IV. CONCLUSIONS

The following main conclusions might be drawn from this analysis: (i) For the  $A = 18-21$  neutron-rich nitrogen isotopes, the main contribution to the ground-state wave function comes from the coupling of  $d_{5/2}$  shell neutrons to the core. For the  $^{18,19}\text{N}$  cases, the valence neutron couples to low-lying excited states, while it couples to the ground state for  $^{20,21}\text{N}$ . An explanation for this might be that the  $d$  state is more pure in the vicinity of  $N = 14$ , while the structures of the lighter isotopes are more complex. (ii) For  $^{22}\text{N}$ , the fit needs similar amounts of  $s_{1/2}$  and  $d_{3/2(5/2)}$  contributions, with the  $s$  contribution coupled to the ground state of the core. This result indicates that the role of the  $s$ -wave neutron is also important here, but much less pronounced than in  $^{23,24}\text{O}$ , where the  $s$  state is dominating. (iii) A clear reduction of the full width at half maximum (FWHM) of the longitudinal-momentum distribution of the fragments in the one-neutron knockout of  $^{22}\text{N}$  with respect to the lighter projectiles is also observed (see Table I and Fig. 2). This reduction directly reflects the change from a  $0d_{5/2}$  valence-neutron configuration to  $1s_{1/2}$  when crossing  $N = 14$ . (iv) These data provide the first measurement of

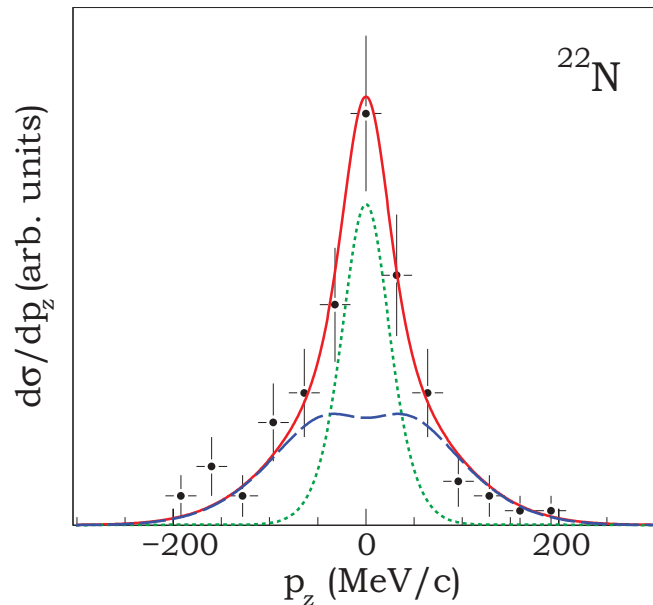


FIG. 2. (Color online) Longitudinal-momentum distributions of fragments after neutron-knockout of  $^{22}\text{N}$ . The curves correspond to theoretical calculations in an eikonal Glauber model folded with the experimental resolution. The dotted and dashed lines correspond to the coupling of the core to an  $s_{1/2}$  and a  $d_{3/2}$  neutron, respectively, and the solid curve to their sum.

one-neutron knockout from the drip-line nucleus  $^{22}\text{N}$ , which has been proposed as a possible one-neutron halo candidate in several papers [25–28]. The more advanced analysis of the data published in Ref. [5] given here, together with earlier results, allows one to conclude that the  $^{22}\text{N}$  ground state exhibits a halo structure. The results also show that the  $N = 14$  subshell in  $^{22}\text{N}$  is somewhat reduced as compared to that of  $^{23}\text{O}$ .

#### ACKNOWLEDGMENTS

This work was supported by: GSI, via Hochschulzusammenarbeitsvereinbarungen under Contracts No. DA RICK,

No. OF ELZ, and No. MZ KRAK; German BMBF; the DFG Cluster of Excellence, Origin and Structure of the Universe; FBR under Contract No. 08-02-012244; EC under Contract No. ERBCHGE-CT92-003; Ministerio de Ciencia e Innovación under Project No. FPA2009-14604-602-01; Ministerio de Educación under Grant No. FPU-AP2005-3308, and the Galician Consellería de Educación e Ordenación Universitaria, Consolidación e Estructuración de Unidades Competitivas 2010/57. T.N. acknowledges support from the Royal Swedish Academy of Sciences via the Knut and Alice Wallenberg Foundation. Financial support from the Swedish Research Council is acknowledged.

- 
- [1] D. Cortina-Gil *et al.*, *Phys. Rev. Lett.* **93**, 062501 (2004).
  - [2] R. Kanungo *et al.*, *Phys. Rev. Lett.* **102**, 152501 (2009).
  - [3] C. R. Hoffman *et al.*, *Phys. Lett. B* **672**, 17 (2009).
  - [4] C. Rodríguez-Tajes *et al.*, *Phys. Lett. B* **687**, 26 (2010).
  - [5] C. Rodríguez-Tajes *et al.*, *Phys. Rev. C* **82**, 024305 (2010).
  - [6] G. D. Westfall *et al.*, *Phys. Rev. Lett.* **43**, 1859 (1979).
  - [7] A. C. Müller *et al.*, *Nucl. Phys. A* **513**, 1 (1990).
  - [8] N. A. Orr *et al.*, *Phys. Lett. B* **258**, 29 (1991).
  - [9] A. Ozawa *et al.*, *Nucl. Phys. A* **673**, 411 (2000).
  - [10] A. Ozawa *et al.*, *Nucl. Phys. A* **691**, 599 (2001).
  - [11] A. Ozawa, T. Suzuki, and I. Tanihata, *Nucl. Phys. A* **693**, 32 (2001).
  - [12] A. Khouaja *et al.*, *Nucl. Phys. A* **780**, 1 (2006).
  - [13] D. Sohler *et al.*, *Phys. Rev. C* **77**, 044303 (2008).
  - [14] M. J. Strongman *et al.*, *Phys. Rev. C* **80**, 021302 (2009).
  - [15] C. S. Sumithrarachchi *et al.*, *Phys. Rev. C* **81**, 014302 (2010).
  - [16] M. Madurga *et al.*, *Phys. Lett. B* **677**, 255 (2009).
  - [17] H. Geissel *et al.*, *Nucl. Instr. Meth. B* **70**, 286 (1992).
  - [18] K. Hencken, G. Bertsch, and H. Esbensen, *Phys. Rev. C* **54**, 3043 (1996).
  - [19] T. Aumann *et al.*, *Phys. Rev. Lett.* **84**, 35 (2000).
  - [20] Y. L. Parfenova, M. V. Zhukov, and J. S. Vaagen, *Phys. Rev. C* **62**, 044602 (2000).
  - [21] Y. L. Parfenova and M. V. Zhukov, *Phys. Rev. C* **66**, 064607 (2002).
  - [22] H. DeVries, C. W. DeJaeger, and C. DeVries, *At. Data Nucl. Data Tables* **36**, 495 (1987).
  - [23] D. R. Tilley, H. R. Weller, and C. M. Cheves, *Nucl. Phys. A* **565**, 1 (1993).
  - [24] M. Wiedeking *et al.*, *Phys. Rev. C* **77**, 054305 (2008).
  - [25] Z. Ren, B. Chen, Z. Ma, Z. Zhu, and G. Xu, *J. Phys. G* **22**, 523 (1996).
  - [26] R. K. Gupta, M. Balasubramaniam, R. K. Puri, and W. Scheid, *J. Phys. G* **26**, 23 (2000).
  - [27] R. K. Gupta, S. Kumar, M. Balasubramaniam, G. Münzenberg, and W. Scheid, *J. Phys. G* **28**, 699 (2002).
  - [28] R. Kanungo, I. Tanihata, and A. Ozawa, *Phys. Lett. B* **512**, 261 (2001).